THE JOURNAL OF BIOLOGICAL CHEMISTRY VOL. 288, NO. 44, pp. 31670–31677, November 1, 2013

Replacement of the Catalytic Nucleophile Aspartyl Residue of Dextran Glucosidase by Cysteine Sulfinate Enhances Transglycosylation Activity

Received for publication, June 4, 2013, and in revised form, September 18, 2013 Published, JBC Papers in Press, September 19, 2013, DOI 10.1074/jbc.M113.491449

Wataru Saburi, Momoko Kobayashi, Haruhide Mori, Masayuki Okuyama, and Atsuo Kimura[1]

From the Research Faculty of Agriculture, Hokkaido University, Sapporo 060-8689, Japan

Background: A mutant dextran glucosidase where the nucleophilic Asp (-COO^-) was replaced by cysteine sulfinate (-SOO^-) was characterized.
Results: The cysteine sulfinate-introduced enzyme showed higher transglucosylation activity than wild type enzyme.
Conclusion: The more acidic nucleophile (-SOO^-) increased transglycosylation activity.
Significance: A novel strategy to enhance transglycosylation by glycosidases is proposed.

Dextran glucosidase from *Streptococcus mutans* (SmDG) catalyzes the hydrolysis of an α-1,6-glucosidic linkage at the nonreducing end of isomaltooligosaccharides and dextran. This enzyme has an Asp-194 catalytic nucleophile and two catalytically unrelated Cys residues, Cys-129 and Cys-532. Cys-free SmDG was constructed by replacement with Ser (C129S/C532S (2CS), the activity of which was the same as that of the wild type, SmDG). The nucleophile mutant of 2CS was generated by substitution of Asp-194 with Cys (D194C-2CS). The hydrolytic activity of D194C-2CS was 8.1×10^{-4} % of 2CS. KI-associated oxidation of D194C-2CS increased the activity up to 0.27% of 2CS, which was 330 times higher than D194C-2CS. Peptide-mapping mass analysis of the oxidized D194C-2CS (Ox-D194C-2CS) revealed that Cys-194 was converted into cysteine sulfinate. Ox-D194C-2CS and 2CS shared the same properties (optimum pH, pI, and substrate specificity), whereas Ox-D194C-2CS had much higher transglucosylation activity than 2CS. This is the first study indicating that a more acidic nucleophile (-SOO^-) enhances transglycosylation. The introduction of cysteine sulfinate as a catalytic nucleophile could be a novel approach to enhance transglycosylation.

Dextran glucosidase (EC 3.2.1.70, DG),[2] which is involved in the metabolism of isomaltooligosaccharides in Streptococci and Lactobacilli, hydrolyzes α-1,6-glucosidic linkages at nonreducing ends of isomaltooligosaccharides and dextran (1, 2). In contrast to oligosaccharide α-1,6-glucohydrases (EC 3.2.1.10), which are specific to short-chain substrates, DG acts on not only short-chain substrates but also long-chain substrates such as dextran.

According to sequence-based classification of glycoside hydrolases (GH) (3, 4), DG is classified into GH 13 subfamily 31. GH 13 consists of ~30 kinds of retaining glycosidases and transglycosylases, including α-amylases (EC 3.2.1.1), cyclodextrin glucanotransferases (EC 2.4.1.19), branching enzymes (EC 2.4.1.18), and α-glucosidases (EC 3.2.1.20) acting on α-glucans such as starch, cyclodextrin, dextran, and sucrose. Despite low sequence similarity of entire sequences, the enzymes of this family share three common domains, A, B, and C. Domain A is the catalytic domain folded in a $(\beta/\alpha)_8$-barrel (5). Domain B is a long loop connecting β-strand 3 and α-helix 3 of domain A. Domain C follows domain A and is made up of β-strands. Four short conserved sequences (I–IV) of GH 13 enzymes are involved in the formation of the catalytic sites.

It is believed that retaining GHs, including DG, catalyze the hydrolysis of glycosidic linkages through a double-displacement mechanism (6), which has been postulated by Koshland (7) (Fig. 1). Generally, two carboxyl groups act as the catalysts, although some exceptions have been reported (8–11). The catalytic carboxylate (catalytic nucleophile) nucleophilically attacks the anomeric carbon to form a covalently bound glycosyl-enzyme intermediate with inverted anomeric configuration. The catalytic carboxyl group (general acid/base catalyst) simultaneously donates a proton to the glycosidic oxygen and releases the aglycone. The dissociated general acid/base catalyst promotes the nucleophilic attack of the oxygen water to the C1 of the intermediate, and the glycone part is released upon a second anomeric inversion. These two steps proceed through an oxocarbenium ion-like transition state. Transglycosylation occurs when the hydroxyl group of a sugar serves as an acceptor of the glycone part. The catalytic nucleophile and general acid/base catalyst of GH family 13 enzymes are Asp and Glu, found in the conserved regions II and III, respectively (5), and these residues are situated at the C-terminal ends of β-strand 4 and β-strand 5 of domain A, respectively.

Recently, we have determined the three-dimensional structures of DG from *Streptococcus mutans* (SmDG, GenBank™ code, BAE79634.1) in the native state (Protein Data Bank code, 2ZIC) and complexed with isomaltotriose (IG3; Protein Data Bank code, 2ZID) (12). Asp-194 and Glu-236, corresponding to

[1] To whom correspondence should be addressed: Research Faculty of Agriculture, Hokkaido University, Kita-9 Nishi-9, Kita-ku, Sapporo 060-8589, Japan. Tel. and Fax: 81-11-706-2808; E-mail: kimura@abs.agr.hokudai.ac.jp.

[2] The abbreviations used are: DG, dextran glucosidase; SmDG, *Streptococcus mutans* DG; 2CS, C129S/C532S; D194C-2CS, D194C/C129S/C532S; GH, glycoside hydrolase; IG2, isomaltose; IG3, isomaltotriose; IG4, isomaltotetraose; IG5, isomaltopentaose; Ox-D194C-2CS, oxidized D194C-2CS; PG, phenyl α-D-glucopyranoside; *p*NPG, *p*-nitrophenyl α-D-glucopyranoside; *p*NPIG2, *p*-nitrophenyl α-isomaltoside.

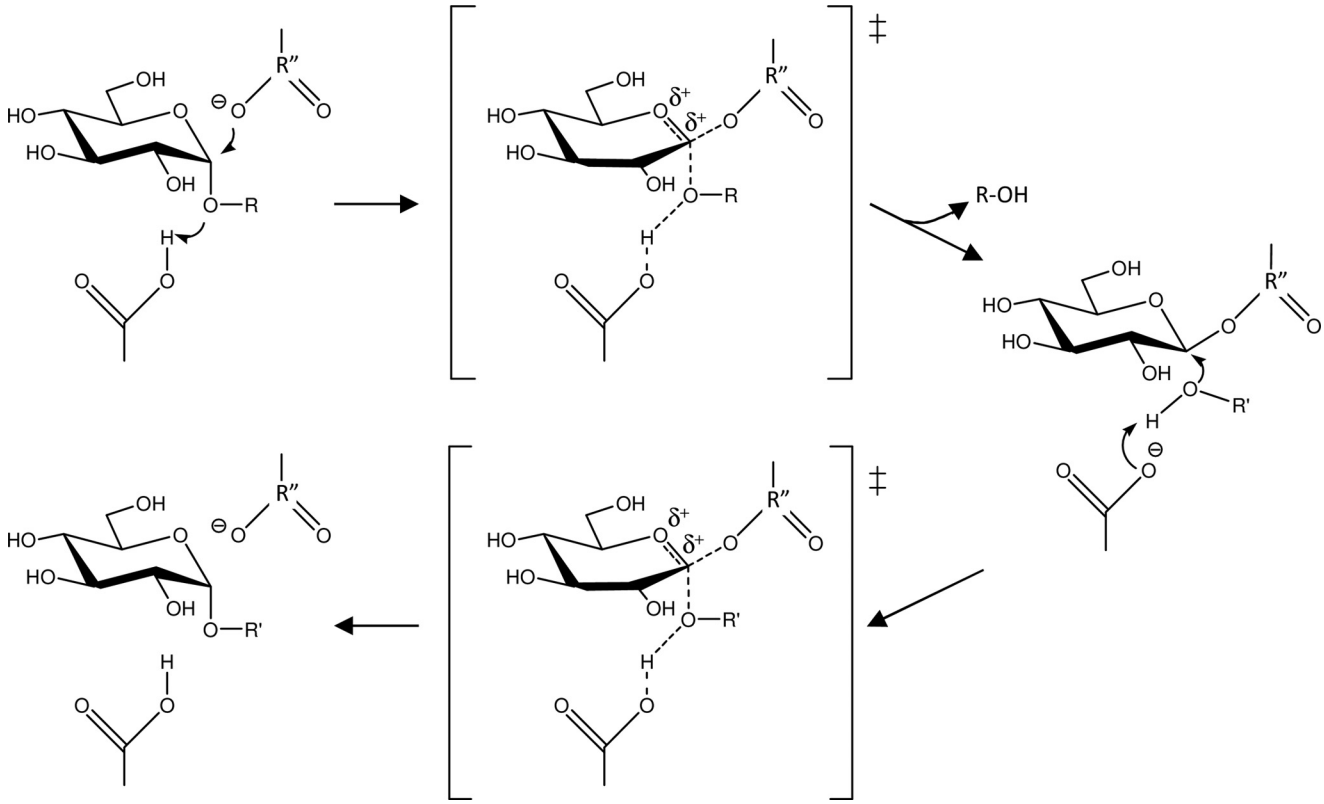

FIGURE 1. **The catalytic mechanisms of retaining glycosidases.** A mechanism for α-glucosidase is shown. *R* indicates the aglycone part. For hydrolysis and transglucosylation, *R′* is the proton and sugar, respectively. The *R″* is the carbon and sulfur, indicating that the nucleophilic residue is Asp and cysteine sulfinate, respectively. *Double dagger* symbols indicate transition state of the reaction.

TABLE 1

Sequences of the primers used in this study

NcoI and XhoI sites are underlined. Substituted nucleotides are double-underlined.

Name	Sequence (5′→3′)	Direction	Purpose
SmDGN	GATACCATGGAAAAACATTGGTGGCAC	Sense	Covering 5′-terminal of the SmDG gene
SmDGC	ATCCTCGAGTATCTTAATACAAAAAGCATC	Antisense	Covering 3′-terminal of the SmDG gene
C129Ss	TATTATATTTGGTCTGACCAGCCAAAT	Sense	Preparation of 2CS
C129Sa	ATTTGGCTGGTCAGACCAAATATAATA	Antisense	Preparation of 2CS
C532Sa	ATCCTCGAGTATCTTAATAGAAAAAGCAT	Antisense	Preparation of 2CS
D194A	GGCTTTCGGATGGCCGTCATTGATATG	Sense	Preparation of D194A
D194C	GGCTTTCGGATGTGCGTCATTGATATG	Sense	Preparation of D194C-2CS

the Asp and Glu conserved in regions II and III, respectively, are located at the bottom of the active site pocket, and they are thought to act as the catalytic nucleophile and the general acid/base catalyst, respectively.

Cysteine sulfinate substitutions of the catalytic carboxylates (general base catalyst) in inverting glycosidases have been reported (13, 14). In the case of GH 15 glucoamylase (EC 3.2.1.3), replacement of the general base catalyst by cysteine sulfinate increased the catalytic activity (the mutant enzymes showed 160% of the activity of the wild type) (13). On the other hand, the mutant GH 6 cellulase harboring cysteine sulfinate in the position of the catalytic base showed only 52% of the wild type activity, but it had higher activity at low pH than the wild type cellulase (14). In contrast to these inverting glycosidases, the effect of sulfinate substitution of a catalytic carboxylate on a retaining glycosidase has not been investigated thus far. In this study, the catalytic nucleophile of SmDG, Asp-194, was replaced by cysteine sulfinate (Fig. 1), and the mutant enzyme was characterized in detail.

EXPERIMENTAL PROCEDURES

Preparation of C129S/C532S (2CS), D194A/C129S/C532S (D194C-2CS), and D194A

Generation of the mutants was as follows. (i) For 2CS, replacement of two original Cys residues (Cys-129 and Cys-532) with Ser was carried out by the overlap extension PCR method (15), in which the expression plasmid of the wild type SmDG (1) as the template was used. (ii) For D194A and D194C-2CS, Asp-194 of wild type enzyme or 2CS was substituted with Ala or Cys by site-directed mutagenesis by the megaprimer PCR method (16), in which the expression plasmid of the wild type enzyme or 2CS was used for D194A or D194C-2CS, respectively. Sequences of the primers used are summarized in Table 1. Amplified PCR fragments were cloned into pET-23d (Novagen, Darmstadt, Germany) as described previously (1). The resulting expression plasmids were introduced into *Escherichia coli* BL21 (DE3) CodonPlus RIL (Stratagene; La Jolla, CA), and the mutant enzymes were prepared as reported else-

where (1). Induction of protein production was carried out at 15 °C for 18 h to improve the production level of the recombinant protein. Concentrations of the purified enzymes were measured by quantification of each amino acid by the ninhydrin colorimetric method using JLC-500/V (Jeol Ltd.; Tokyo, Japan) after hydrolysis of 32 μg of the purified enzymes in 6 N HCl at 110 °C for 24 h (17).

Oxidation of D194C-2CS

The thiol group of Cys-194 of D194C-2CS was oxidized by KI (13, 14). 2CS, as a control, was also treated under the same conditions. To determine the optimum concentration of KI treatment, a mixture (100 μl) containing 0–0.3 M KI, 10 μM bromine, 0.25 M sodium phosphate buffer (pH 6.0), and 3.16 μM D194C-2CS or 3.51 μM 2CS was incubated at 25 °C for 30 h, and the activity was measured as described herein.

The oxidized D194C-2CS (Ox-D194C-2CS) was prepared on a large scale. Fifty ml of a mixture containing 0.2 M KI and the above-mentioned components was incubated at 25 °C for 240 h and dialyzed thoroughly against 20 mM sodium phosphate buffer (pH 6.0). The thiol group of D194C-2CS before and after oxidation was quantified by Ellman's method (18) The sample (3.46 nmol) was dried up *in vacuo* and dissolved in 90 μl of 0.1 M Tris-HCl buffer (pH 7.0) containing 10 mM EDTA and 6 M guanidine-HCl. Ten μl of 50 mM sodium phosphate buffer (pH 7.0) containing 4 mM 5,5′-dithiobis(2-nitrobenzoic acid) was added and incubated at room temperature for 10 min. Liberated 3-carboxy-4-nitrothiophenolate ion from 5,5′-dithiobis(2-nitrobenzoic acid) was measured on the basis of $\epsilon_{1\ m,\ 412\ nm} = 13{,}380$ (19).

Structural Analysis of Oxidized Cys

One nmol of Ox-D194C-2CS was dissolved in 100 μl of 0.5 M Tris-HCl buffer (pH 7.5) containing 10 mM EDTA, 4 M urea, and 0.2 μM lysyl endopeptidase (Wako Pure Chemical Industries; Osaka, Japan), and incubated at 37 °C for 24 h. The resulting mixture was purified using HPLC under following conditions: column, Capcell Pak C_{18} UG120 (ϕ4.6 × 150 mm: Shiseido; Tokyo, Japan); column temperature, 50 °C; elution, 0–50% acetonitrile linear gradient in 0.1% trifluoroacetic acid; flow rate, 1 ml/min; detection, absorbance at 214 nm. To screen the peptide containing oxidized Cys-194, the molecular masses of the separated peptides were measured by matrix-assisted laser desorption ionization-time of flight-mass spectrometry with the Voyager-DE-STR TOF-MS system (Applied Biosystems, Foster City, CA). As a matrix solution, 32.5 mM 2,5-dihydroxybenzoic acid in 30% acetonitrile and 0.1% trifluoroacetic acid was used. The sequence of the peptide was confirmed using a Procise 491 protein sequencer (Applied Biosystems).

The pI values of 2CS, D194C-2CS, and Ox-D194C-2CS were measured by isoelectric focusing electrophoresis. Two hundred nanograms of each protein was applied on a PhastGel IEF 4-6.5 (Amersham Biosciences), and the electrophoresis was performed using a PhastSystem (Amersham Biosciences). Protein was detected by Coomassie Brilliant Blue staining using Rapid CBB Kanto (Kanto Kagaku, Tokyo, Japan).

Enzyme Assay

In the standard enzyme assay, the activity toward 2 mM *p*-nitrophenyl α-d-glucopyranoside (*p*NPG, Nacalai Tesque, Kyoto, Japan) was measured as described previously (1). Thermal and pH stabilities and optimum pH were evaluated according to our previous study (1). Steady state kinetic parameters for *p*NPG, phenyl α-glucopyranoside (PG) (synthesized by Trevelyan's method (20)), and *p*-nitrophenyl α-isomaltoside (*p*NPIG2) (prepared by our previous method (1)) were determined according to the procedures described previously (21). The kinetic parameters for isomaltose (IG2; Tokyo Kasei, Tokyo) were calculated with some modifications as described below. The transglucosylation ratio (%) was calculated from the division of transglucosylation velocity by aglycone releasing velocity (sum of transglucosylation and hydrolysis). Conditions of the assay are described below.

pNPG—Aglycone releasing and hydrolytic velocities toward 0.2–8 mM *p*NPG were measured as described previously (21), except that EDTA was not added to the reaction mixture. The concentrations of Ox-D194C-2CS, 2CS, and wild type were 192, 0.789, and 0.404 nM, respectively.

PG—The reactions in the presence of 1–20 mM PG were carried out similar to those of *p*NPG except for the substrate and enzyme concentrations. The concentrations of Ox-D194C-2CS and 2CS were 30.8 and 0.980 nM, respectively. The liberated glucose was measured by the glucose oxidase-peroxidase method to determine the hydrolytic velocity (22). For the measurement of aglycone releasing velocity, liberated phenol was quantified by the method of Robertson and Halvorson (23).

pNPIG2—A reaction mixture (50 μl) containing 2.56 nM Ox-D194C-2CS or 0.196 nM 2CS, 1–4.5 mM *p*NPIG2, 40 mM sodium phosphate buffer (pH 6.0), and 0.02% BSA was incubated at 37 °C for 10 min. The reaction was stopped by adding 5 μl of 5 M acetic acid, and the mixture was separated by HPLC to quantify *p*NPG (aglycone) and *p*-nitrophenyl α-isomaltotrioside (transglucosylation product). The HPLC conditions were as follows: column, ϕ4.6 × 250 mm AP303 (YMC; Kyoto, Japan); column temperature, 50 °C; eluent, 9% acetonitrile; flow rate, 1 ml/min; detection, absorbance at 313 nm.

IG2—In the reaction to IG2, glucose was liberated as the hydrolytic product (glycone part) and the leaving group of both transglucosylation and hydrolysis. Thus the velocity of glucose liberation (v_g) was given by sum of velocities for leaving group release (v_{lr}) and hydrolysis (v_h). From our previous study (21), v_{lr} and v_h were calculated as follows

$$v_{lr} = (k_{cat1}K_{m2}[S] + k_{cat2}[S]^2)/([S]^2 + K_{m2}[S] + K_{m1}K_{m2}) \quad \text{(Eq. 1)}$$

$$v_h = k_{cat1}K_{m2}[S]/([S]^2 + K_{m2}[S] + K_{m1}K_{m2}) \quad \text{(Eq. 2)}$$

and therefore v_g was given as follows

$$v_g = v_{lr} + v_h = (2k_{cat1}K_{m2}[S] + k_{cat2}[S]^2)/([S]^2 + K_{m2}[S] + K_{m1}K_{m2}) \quad \text{(Eq. 3)}$$

A reaction mixture (50 μl) containing 64 nM Ox-D194C-2CS or 0.156 nM 2CS, 1–20 mM IG2, 40 mM sodium phosphate

TABLE 2
Multiple-alignment of the conserved region II of GH 13

Enzyme	Origin	Sequence[a]	Position	Accession[b]
Dextran glucosidase	*Streptococcus mutans*	GFRM**D**VIDM	190–198	Q99040
Oligo-1,6-glucosidase	*Bacillus cereus*	GFRM**D**VINF	195–203	P21332
α-Glucosidase	*Saccharomyces cerevisiae*	GFRI**D**TAGL	210–218	P38158
α-Amylase	*Aspergillus oryzae*	GLRI**D**TVKH	223–231	Q00250
	Sus scrofa (pancreatic)	GFRI**D**ASKH	193–201	P00690
	Homo sapiens (pancreatic)	GFRL**D**ASKH	208–216	P04746
Neopullulanase	*Geobacillus stearothermophilus*	GWRL**D**VANE	324–332	P38940
Isoamylase	*Pseudomonas amyloderamosa*	GFRF**D**LASV	397–405	P10342
Branching enzyme	*Escherichia coli*	ALRV**D**AVAS	401–409	P07762
CGTase[c]	*Bacillus circulans* 251	GIRM**D**AVKH	252–260	P43379
Amylosucrase	*Neisseria polysaccharea*	ILRM**D**AVAF	290–298	Q9ZEU2

[a] Bold letters indicate the catalytic nucleophile.
[b] UniProtKB databank accession numbers are shown.
[c] CGTase, cyclodextrin glycosyltransferase.

buffer (pH 6.0), and 0.02% BSA was incubated at 37 °C for 10 min. Liberated glucose was measured as described above.

TLC Analysis of Products from IG2 and IG3

The reactions to IG2 and IG3 by Ox-D194C-2CS and 2CS were analyzed. One ml of a mixture consisting of 192 nM Ox-D194C-2CS or 19.2 nM 2CS, 20 mM IG2, or 10 mM IG3 (Seikagaku, Tokyo, Japan) and 10 mM sodium phosphate buffer (pH 6.0) was incubated at 37 °C. An aliquot (100 μl) was taken at the time indicated and immediately boiled for 3 min. The resulting mixture (2 μl) was analyzed by TLC. 2-Propanol/1-butanol/water, v/v/v, 12:3:4 was used as the developing solvent. The chromatogram was visualized with a detection reagent (5% sulfuric acid in ethanol) followed by heating at 120 °C.

Product Distribution Analysis of Reaction toward IG3

Reaction products from IG3 were quantified by high performance anion exchange chromatography. A reaction mixture (500 μl) consisting of 19.2 nM 2CS or 1.92 μM Ox-D194C-2CS, 10 mM IG3, and 10 mM sodium phosphate buffer (pH 6.0) was incubated at 37 °C. An aliquot (50 μl) was taken at the indicated time and heated at 100 °C for 10 min to stop the reaction. High performance anion exchange chromatography was carried out under the following conditions: column, CarboPac PA1 (ϕ4.0 × 250 mm, Dionex, Sunnyvale, CA); injection volume, 10 μl; eluent, 320 mM NaOH; flow rate, 0.8 ml/min; detection, pulsed amperometry.

RESULTS AND DISCUSSION

Characterization of D194A Mutant—To confirm the importance of Asp-194 for SmDG catalytic activity, D194A was characterized. From 1 liter of culture fluid of the *E. coli* transformant, 31.8 mg of purified D194A was obtained. The enzyme activity significantly decreased upon substitution of Asp-194 to Ala, and its specific activity was 6.70×10^{-4} units/mg (3.9×10^{-4} % of wild type). This indicates that as the catalytic nucleophile, Asp-194 is essential for enzyme activity as predicted from the structural analysis of SmDG (12) and comparison of its amino acid sequence with those GH 13 enzymes where the catalytic nucleophiles have been demonstrated experimentally (24–28) (Table 2).

Production of 2CS—Two Cys residues of SmDG, Cys-129 and Cys-532, were replaced by Ser, generating a Cys-free SmDG, *i.e.* 2CS. From 1 liter of culture medium, 20.1 mg of purified 2CS was recovered. The specific activity toward 2 mM *p*NPG of 2CS was 160 units/mg, which was similar to that of the wild type SmDG, 171 units/mg (1). 2CS showed the same pH optimum (pH 6.0), pH stability (pH 5.6–7.0 at 37 °C for 15 min), thermal stability (≤40 °C at pH 6.0 for 15 min), and substrate specificity as wild type SmDG (1). Kinetic parameters of 2CS for *p*NPG were also basically close to those of the wild type (Table 3). The substitutions of two Cys residues with Ser did not affect the enzymatic properties, and 2CS was used as the control enzyme in the following analyses.

TABLE 3
Kinetic parameters of Ox-D194C-2CS and 2CS
Reaction velocities were measured at 37°C at pH 6.0 (sodium phosphate buffer). N.D, not determined. Data are mean ± S.D. deviation for three independent experiments.

Ox-D194C-2CS					
Substrate	k_{cat1} (s^{-1})	k_{cat2} (s^{-1})	K_{m1} (mM)	K_{m2} (mM)	K_{TG} (mM)
*p*NPG	0.0620 ± 0.0043	0.755 ± 0.048	0.116 ± 0.039	0.889 ± 0.050	0.073
PG	0.958 ± 0.472	29.5 ± 1.0	0.688 ± 0.645	7.60 ± 4.82	0.247
*p*NPIG2	36.0 ± 10.3	108 ± 7	0.314 ± 0.283	4.33 ± 2.37	1.44
IG2	4.75 ± 0.18	78.4 ± 6.6	5.12 ± 0.18	99.3 ± 10.9	6.02
2CS					
Substrate	k_{cat1} (s^{-1})	k_{cat2} (s^{-1})	K_{m1} (mM)	K_{m2} (mM)	K_{TG} (mM)
*p*NPG	187 ± 13	196 ± 1	0.312 ± 0.260	1.55 ± 0.31	1.48
PG	294 ± 16	795 ± 22	1.32 ± 0.54	7.94 ± 1.37	2.94
*p*NPIG2	601 ± 135	194 ± 4	1.53 ± 0.95	4.41 ± 3.68	13.7
IG2	N.D.	N.D.	N.D.	N.D.	N.D.
Wild type					
Substrate	k_{cat1} (s^{-1})	k_{cat2} (s^{-1})	K_{m1} (mM)	K_{m2} (mM)	K_{TG} (mM)
*p*NPG	157 ± 23	220 ± 8	0.501 ± 0.074	1.58 ± 0.31	1.13

Oxidation of the Thiol Group of D194C-2CS—D194C-2CS, in which Asp-194 of 2CS was replaced by Cys, was prepared from 2 liters of culture broth of the *E. coli* transformant, and 34.9 mg of purified enzyme was obtained. The specific activity of D194C-2CS was 1.30×10^{-3} units/mg, which was 8.1×10^{-4} % of 2CS.

To oxidize the thiol group of Cys-194, D194C-2CS was treated with various concentrations of KI at 25 °C for 30 h. The activity of D194C-2CS increased depending on the concentration of KI up to 0.3 M (Fig. 2*a*). Using 2CS as a control, the activity was not changed by incubation with ≤0.2 M KI and decreased to 71% of the original activity in the presence of 0.3 M KI. When D194C-2CS was incubated in the presence of 0.2 M KI, the maximal activity was reached at 195 h and did not

change significantly upon further incubation, whereas the activity of 2CS did not change when incubated under the same conditions for 300 h (Fig. 2*b*). To prepare Ox-D194C-2CS for characterization, 158 nmol of D198C-2CS was treated with 0.2 M KI for 240 h at 25 °C. After the incubation, no free thiol group was detected in 3.46 nmol of Ox-D194C-2CS, indicating that the single Cys at the catalytic center was fully oxidized (more than 95% of D194C-2CS was oxidized, estimated from the limit of detection of free-thiol group).

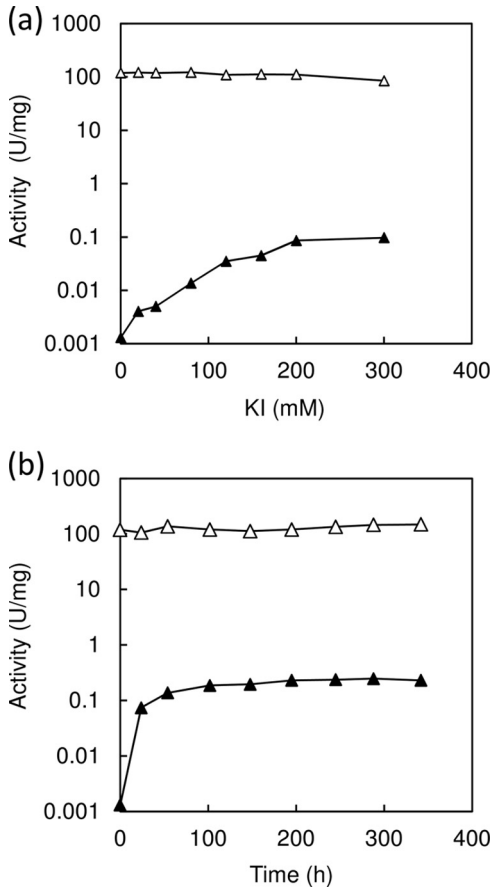

FIGURE 2. **Oxidation of D194C-2CS with KI.** *a*, oxidation of D194C-2CS with various concentrations of KI. *Filled* and *open triangles* indicate D194C-2CS and 2CS, respectively. *b*, time course of oxidation of D194C-2CS with 0.2 M KI. *Filled* and *open triangles* indicate D194C-2CS and 2CS, respectively.

The structure of the oxidized thiol group was analyzed by mass spectrometry. After digestion of Ox-D194C-2CS with lysyl endopeptidase, the resulting peptides were separated by HPLC, and the mass of each peptide was measured by matrix-assisted laser desorption ionization-time of flight-mass spectrometry. One peptide of 1629.6 Da was revealed to be Gly-187–Lys-201 by complete Edman degradation sequencing. The mass of this peptide was higher than its theoretical mass of 1596.8 Da by ~32 Da, indicating that Cys-194 was converted to cysteine sulfinate as reported previously for two inverting glycosidases (13, 14). Masses of 17 peptides were assigned, and 35% of the entire sequence was covered. The peptide carrying nonoxidized Cys-194 was not found in the analysis. Although retaining and inverting glycosidases employ distinct reaction mechanisms, the sulfinate group can replace carboxylates, which act as the catalytic nucleophile and general base catalyst in retaining and inverting glycosidases, respectively.

Characterization of Ox-D194C-2CS—The specific activity of Ox-D194C-2CS toward 2 mM *p*NPG was 0.438 units/mg, which was 0.27% of 2CS and 340-fold higher than D194C-2CS. Ox-D194C-2CS was stable from pH 6.0 to 7.0 and at temperatures ≤37 °C. Ox-D194C-2CS was slightly less stable at low pH and high temperature than 2CS. Ox-D194C-2CS showed the highest activity at pH 6.0 toward 0.5 mM IG2, similar to 2CS, and no shift of its pH profile was observed, although introduction of a cysteine sulfinate at the catalytic base position of a cellulase is known to induce an acidic shift in its pH profile (14). Isoelectric focusing electrophoresis of 2CS, D194C-2CS, and Ox-D194C-2CS in the native state revealed that the isoelectric points of all SmDG variants were the same, 5.1, and thus, the replacement of Asp-194 by cysteine sulfinate did not affect its pI. Ox-D194C-2CS acted on only IG2, but not on trehalose, kojibiose, nigerose, and maltose, similar to the activity profile for 2CS, indicating that the substrate preference of Ox-D194C-2CS was the same as that of 2CS.

Transglucosylation Activity of Ox-D194C-2CS—The reactions catalyzed by Ox-D194C-2CS and 2CS to IG3 were monitored by TLC and high performance anion exchange chromatography (Figs. 3*a* and 4). In the initial stage of the reaction, glucose and isomaltotetraose (IG4) were liberated by hydrolysis and transglycosylation, respectively. IG2 was produced by both

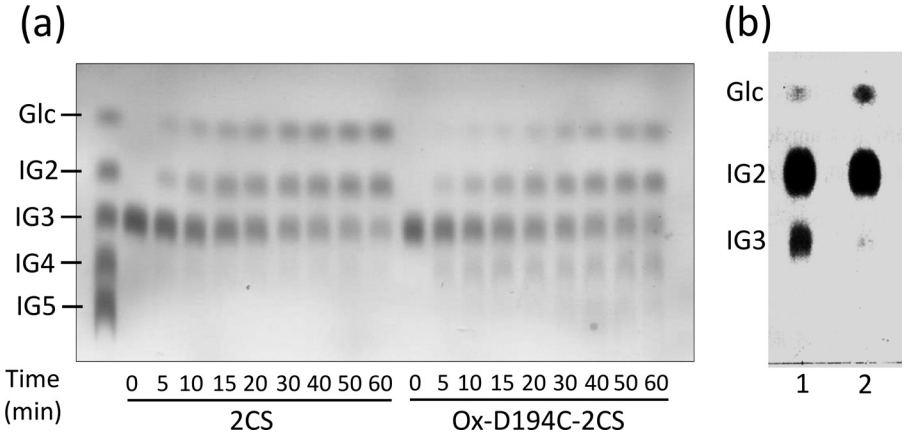

FIGURE 3. **Time course of reaction of Ox-D194C-2CS and 2CS with 10 mM IG3 (*a*) and 20 mM IG2 (*b*).** *IG2–IG5* indicate isomaltose to isomaltoheptaose, respectively. *a*, reaction time and SmDG variants are shown below the chromatogram. *b*, *lane 1*, Ox-D194C-2CS; *lane 2*, 2CS; reaction time, 30 min.

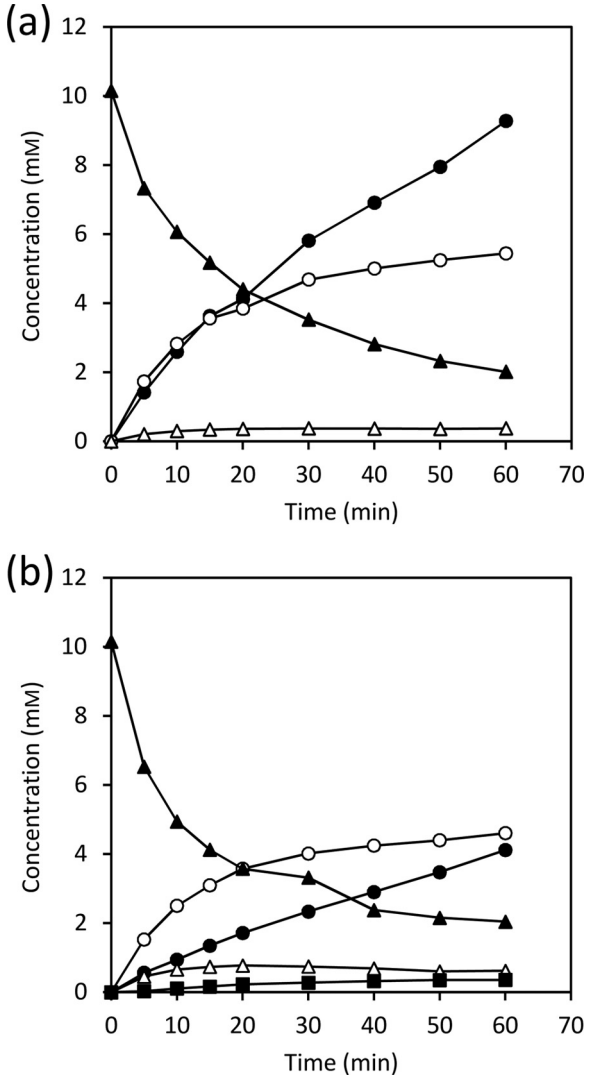

FIGURE 4. **Quantitative analysis of reactions of Ox-D194C-2CS and 2CS with 10 mM IG3.** *Filled circles*, glucose; *open circles*, IG2; *filled triangles*, IG3; *open triangles*, IG4; *filled squares*, IG5. *a*, 2CS. *b*, Ox-D194C-2CS.

reactions. Under the experimental conditions (10 mM IG3), 2CS released an almost equal amount of glucose and IG2 at the initial stage of the reaction (up to 20 min), whereas Ox-D194C-2CS generated not only glucose and IG2 also IG4. This result indicates that 2CS predominantly catalyzed hydrolysis, but Ox-D194C-2CS catalyzed both hydrolysis and transglucosylation. The production level of IG4 reached maximum (0.77 mM) at 20 min of reaction, and the concentration of IG4 was decreased by further incubation. Ox-D194C-2CS also produced a small amount of isomaltopentaose (IG5), which was not detected in the 2CS reaction. The IG5 produced gradually increased during the reaction, and the concentration reached 0.35 mM at 60 min of reaction.

To kinetically analyze the enhancement of transglucosylation, the velocity of aglycone release (the sum of transglucosylation and hydrolysis) and the hydrolysis (transglucosylation for *p*NPIG2) velocity toward *p*NPG, PG, and *p*NPIG2 were measured, and steady state kinetic parameters were determined (Table 3). Ox-D194C-2CS showed 17–3,000-fold lower k_{cat1} values for *p*NPG, PG, and *p*NPIG2 than 2CS, but k_{cat2} values, which are the reaction rate constants at infinite substrate concentration, for these substrates were 1.8–260-fold lower. In particular, Ox-D194C-2CS showed a k_{cat2} value for *p*NPIG2 approximately half of that of 2CS. For Ox-D194C-2CS, the k_{cat1}/k_{cat2} values for *p*NPG, PG, and pNPIG2 were 0.0821, 0.00563, and 0.333, respectively, which were 9.4–66-fold lower than those of 2CS (0.954, 0.370, and 3.10, respectively). Ox-D194C-2CS exhibited lower k_{cat1}/k_{cat2} values than 2CS and similar K_{m2} values, resulting in lower K_{TG} values than 2CS. The K_{TG} value is equal to the substrate concentration giving 50% of the transglucosylation ratio, where the transglucosylation ratio is represented by the following equation (21)

$$\text{Transglucosylation ratio} = v_{tg}/v_{lr} = [S]/(K_{TG} + [S]) \times 100 \quad \text{(Eq. 4)}$$

where

$$K_{TG} = k_{cat1}K_{m2}/k_{cat2} \quad \text{(Eq. 5)}$$

The Ox-D194C-2CS and 2CS transglucosylation ratios for *p*NPG, PG, and *p*NPIG2 increased depending on the substrate concentrations, and all fit the theoretical curves (Fig. 5), which were calculated from the values in Table 3. Ox-D194C-2CS showed considerably higher transglucosylation ratios for these substrates at any substrate concentration tested. When *p*NPG and PG were employed as substrates, Ox-D194C-2CS reached almost 100% of the transglucosylation ratios at concentrations of 4 mM or higher, whereas the transglucosylation ratios of 2CS for these substrates were 75 and 55% at 4 mM, respectively. When compared with 2CS, Ox-D194C-2CS also showed a much higher transglucosylation ratio toward *p*NPIG2, although the substrate concentration tested was not sufficient to reach 100%. The transglucosylation ratios of Ox-D194C-2CS and 2CS for 4.5 mM *p*NPIG2 were 80 and 28%, respectively.

In the reaction to IG2, TLC analysis indicated that Ox-D194C-2CS produced a large amount of IG3 in contrast to 2CS (Fig. 3*b*). Kinetic analysis supported this observation. The velocities of Ox-D194C-2CS for the glucose liberation fitted well to the theoretical curve obtained from Equation 3 (kinetic parameters are shown in Table 3). In contrast to Ox-D194C-2CS, the velocities of 2CS for glucose liberation did not obey Equation 3 and fitted instead to the Michaelis-Menten equation because of a low level of transglucosylation velocity. The k_{cat} ($422 \pm 15\ s^{-1}$) and K_m (7.75 ± 0.56 mM) were similar to the Michaelis-Menten values from our previous data of the wild type (k_{cat}, $483\ s^{-1}$; K_m, 9.35 mM) (1).

Transglucosylation product-formation analysis (Figs. 3 and 4) and small K_{TG} values (Table 3) revealed that Ox-D194C-2CS exhibited significantly higher preference for transglucosylation than 2CS. In other words, the conversion of the catalytic carboxylate (pK_a, 3.90) to a sulfinate (pK_a, 1.50) (29) enhanced preference for transglucosylation. This indicates that, in the deglycosylation step, Ox-D194C-2CS used acceptor sugars more than water (*i.e.* catalytic water). We have no reasonable explanation for this phenomenon, and three-dimensional structural analysis is required to provide structural insight. One possible explanation was that the glucosyl enzyme intermediate was stabilized by changing the nucleophilic carboxylate to sul-

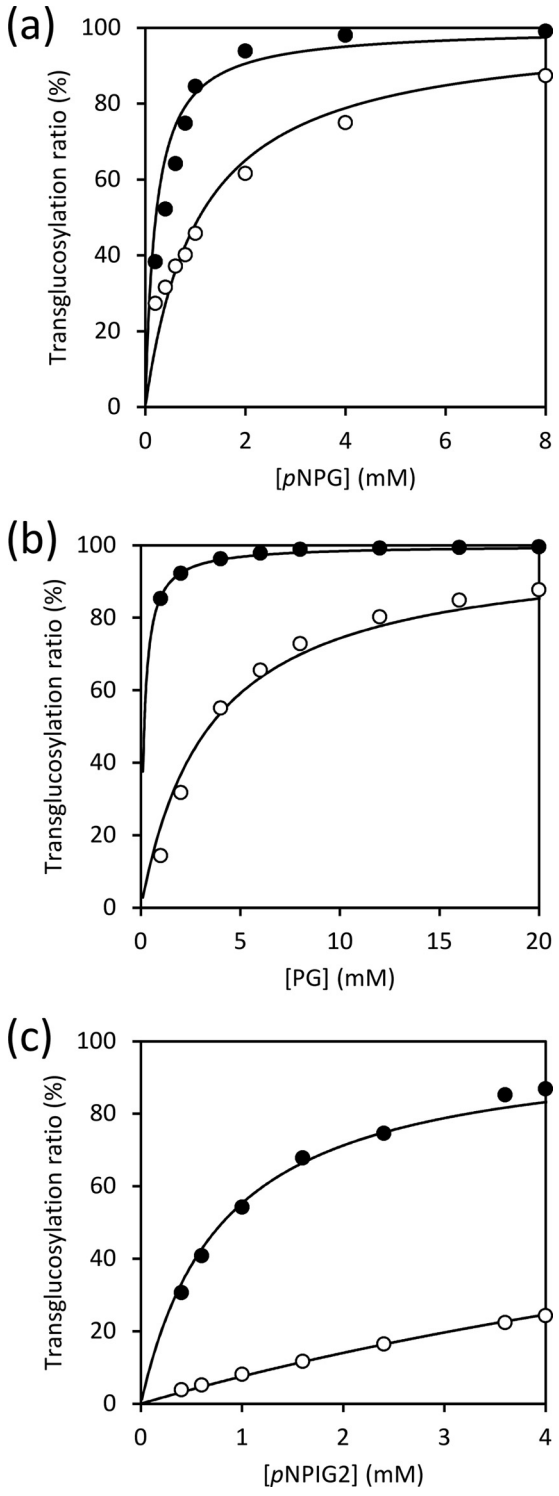

FIGURE 5. **Transglucosylation ratios of Ox-D194C-2CS and 2CS.** *a–c*, transglucosylation ratios for *p*NPG (*a*), PG (*b*), and *p*NPIG2 (*c*) were measured. The *solid line* was generated by fitting to the theoretical equation (21) using the data in Table 3. *Filled* and *open circles* indicate Ox-D194C-2CS and 2CS, respectively.

finate. Sugar binding to the acceptor site of Ox-D194C-2CS might stabilize the transition state of the deglucosylation step and lower the activation barrier increased through stabilization of the glucosyl enzyme intermediate. A similar phenomenon has been observed in the reactivation of glycosyl enzyme intermediates trapped with 5- or 2-fluoroglycoside (30, 31), although in this case, the activation energy of the deglycosylation step increased through destabilization of the transition state by substitution of the hydroxy group of the glycone part to fluorine. The intermediates were fully stable in water so that the labeled positions could be analyzed, but the bound fluoroglycosides were released by the addition of sugars through transglycosylations. This reactivation was thought to be driven by the binding energy between the intermediate and the added acceptor sugar, which was used to stabilize the transition state for the transfer of the glycosyl residue (32).

Ox-D194C-2CS efficiently transferred a glucose moiety not only from aryl glucoside substrates (*p*NPG and PG), but also from natural α-1,6-glucosyl-linked substrates (IG2, IG3, and *p*NPIG2) (Figs. 3–5 and Table 3). Ox-D194C-2CS did not require activated substrates equipped with a good leaving group such as fluorine or dinitrophenolate for efficient transglucosylation. This is useful for the industrial production of oligosaccharides because it is too difficult to employ synthetic substrates in the industrial process. Thus, introduction of cysteine sulfinate as the catalytic nucleophile of retaining glycosidases could be a new strategy to provide high transglycosylation activity. A change of distance between the catalytic nucleophile and general acid/base catalyst results in a large loss of enzyme activity (33). Hence this technique is presumably limited to retaining glycosidases having Asp as the catalytic nucleophile because conversion of Glu into cysteine sulfinate shortens the distance between the catalytic residues.

REFERENCES

1. Saburi, W., Mori, H., Saito, S., Okuyama, M., and Kimura, A. (2006) Structural elements in dextran glucosidase responsible for high specificity to long chain substrate. *Biochim. Biophys. Acta* **1764,** 688–698
2. Møller, M. S., Fredslund, F., Majumder, A., Nakai, H., Poulsen, J. C., Lo Leggio, L., Svensson, B., and Abou Hachem, M. (2012) Enzymology and structure of the GH13_31 glucan 1,6-α-glucosidase that confers isomaltooligosaccharide utilization in the probiotic *Lactobacillus acidophilus* NCFM. *J. Bacteriol.* **194,** 4249–4259
3. Henrissat, B., and Davies, G. (1997) Structural and sequence-based classification of glycoside hydrolases. *Curr. Opin. Struct. Biol.* **7,** 637–644
4. Stam, M. R., Danchin, E. G., Rancurel, C., Coutinho, P. M., and Henrissat, B. (2006) Dividing the large glycoside hydrolase family 13 into subfamilies: towards improved functional annotations of α-amylase-related proteins. *Protein Eng. Des. Sel.* **19,** 555–562
5. MacGregor, E. A., Janecek, S., and Svensson, B. (2001) Relationship of sequence and structure to specificity in the α-amylase family of enzymes. *Biochim. Biophys. Acta* **1546,** 1–20
6. Rye, C. S., and Withers, S. G. (2000) Glycosidase mechanisms. *Curr. Opin. Chem. Biol.* **4,** 573–580
7. Koshland, D. E. (1953) Stereochemistry and the mechanism of enzymatic reactions. *Biol. Rev.* **28,** 416–436
8. Watts, A. G., Damager, I., Amaya, M. L., Buschiazzo, A., Alzari, P., Frasch, A. C., and Withers, S. G. (2003) *Trypanosoma cruzi* trans-sialidase operates through a covalent sialyl-enzyme intermediate: tyrosine is the catalytic nucleophile. *J. Am. Chem. Soc.* **125,** 7532–7533
9. Marković-Housley, Z., Miglierini, G., Soldatova, L., Rizkallah, P. J., Müller, U., and Schirmer, T. (2000) Crystal structure of hyaluronidase, a major allergen of bee venom. *Structure Fold Des.* **8,** 1025–1035
10. Terwisscha van Scheltinga A. C., Armand, S., Kalk, K. H., Isogai, A., Henrissat, B., and Dijkstra, B. W. (1995) Stereochemistry of chitin hydrolysis by a plant chitinase/lysozyme and x-ray structure of a complex with allosamidin: evidence for substrate assisted catalysis. *Biochemistry* **34,** 15619–15623

11. Lodge, J. A., Maier, T., Liebl, W., Hoffmann, V., and Sträter, N. (2003) Crystal structure of *Thermotoga maritima* α-glucosidase AglA defines a new clan of NAD+-dependent glycosidases. *J. Biol. Chem.* **278,** 19151–19158
12. Hondoh, H., Saburi, W., Mori, H., Okuyama, M., Nakada, T., Matsuura, Y., and Kimura, A. (2008) Substrate recognition mechanism of α-1,6-glucosidic linkage hydrolyzing enzyme, dextran glucosidase from *Streptococcus mutans*. *J. Mol. Biol.* **378,** 913–922
13. Fierobe, H. P., Mirgorodskaya, E., McGuire, K. A., Roepstorff, P., Svensson, B., and Clarke, A. J. (1998) Restoration of catalytic activity beyond wild-type level in glucoamylase from *Aspergillus awamori* by oxidation of the Glu400→Cys catalytic-base mutant to cysteinesulfinic acid. *Biochemistry* **37,** 3743–3752
14. Cockburn, D. W., Vandenende, C., and Clarke, A. J. (2010) Modulating the pH-activity profile of cellulase by substitution: replacing the general base catalyst aspartate with cysteinesulfinate in cellulase A from *Cellulomonas fimi*. *Biochemistry* **49,** 2042–2050
15. Ho, S. N., Hunt, H. D., Horton, R. M., Pullen, J. K., and Pease, L. R. (1989) Site-directed mutagenesis by overlap extension using the polymerase chain reaction. *Gene* **77,** 51–59
16. Sarkar, G., and Sommer, S. S. (1990) The "megaprimer" method of site-directed mutagenesis. *BioTechniques* **8,** 404–407
17. Moore, S., and Stein, W. H. (1948) Photometric ninhydrin method for use in the chromatography of amino acids. *J. Biol. Chem.* **176,** 367–388
18. Ellman, G. L. (1959) Tissue sulfhydryl groups. *Arch. Biochem. Biophys.* **82,** 70–77
19. Gething, M. J. H., and Davidson, B. E. (1972) The molar absorption coefficient of reduced Ellman's reagent: 3-carboxylato-4-nitro-thiophenolate. *Eur. J. Biochem.* **30,** 352–353
20. Trevelyan, W. E. (1966) Preparation of phenyl and *p*-nitrophenyl α-D-glucopyranosides for use in the assay of yeast maltase. *Carbohydr. Res.* **2,** 418–420
21. Kobayashi, M., Hondoh, H., Mori, H., Saburi, W., Okuyama, M., and Kimura, A. (2011) Calcium ion-dependent increase in thermostability of dextran glucosidase from *Streptococcus mutans*. *Biosci. Biotechnol. Biochem.* **75,** 1557–1563
22. Miwa, I., Okudo, J., Maeda, K., and Okuda, G. (1972) Mutarotase effect on colorimetric determination of blood glucose with -D-glucose oxidase. *Clin. Chim. Acta* **37,** 538–540
23. Robertson, J. J., and Halvorson, H. O. (1957) The components of maltozymase in yeast, and their behavior during deadaptation. *J. Bacteriol.* **73,** 186–198
24. McCarter, J. D., and Withers, S. G. (1996) Unequivocal identification of Asp-214 as the catalytic nucleophile of *Saccharomyces cerevisiae* α-glucosidase using 5-fluoro glycosyl fluorides. *J. Biol. Chem.* **271,** 6889–6894
25. Mosi, R., He, S., Uitdehaag, J., Dijkstra, B. W., and Withers, S. G. (1997) Trapping and characterization of the reaction intermediate in cyclodextrin glycosyltransferase by use of activated substrates and a mutant enzyme. *Biochemistry* **36,** 9927–9934
26. Rydberg, E. H., Li, C., Maurus, R., Overall, C. M., Brayer, G. D., and Withers, S. G. (2002) Mechanistic analyses of catalysis in human pancreatic α-amylase: detailed kinetic and structural studies of mutants of three conserved carboxylic acids. *Biochemistry* **41,** 4492–4502
27. Uitdehaag, J. C., Mosi, R., Kalk, K. H., van der Veen, B. A., Dijkhuizen, L., Withers, S. G., and Dijkstra, B. W. (1999) X-ray structures along the reaction pathway of cyclodextrin glycosyltransferase elucidate catalysis in the α-amylase family. *Nat. Struct. Biol.* **6,** 432–436
28. Brzozowski, A. M., and Davies, G. J. (1997) Structure of the *Aspergillus oryzae* α-amylase complexed with the inhibitor acarbose at 2.0 Ä resolution. *Biochemistry* **36,** 10837–10845
29. Palmieri, F., Stipani, I., and Iacobazzi, V. (1979) The transport of L-cysteinesulfinate in rat liver mitochondria. *Biochim. Biophys. Acta* **555,** 531–546
30. Braun, C., Lindhorst, T., Madsen, N. B., and Withers, S. G. (1996) Identification of Asp 549 as the catalytic nucleophile of glycogen-debranching enzyme via trapping of the glycosyl-enzyme intermediate. *Biochemistry* **35,** 5458–5463
31. Blanchard, J. E., and Withers, S. G. (2001) Rapid screening of the aglycone specificity of glycosidases: applications to enzymatic synthesis of oligosaccharides. *Chem. Biol.* **8,** 627–633
32. Street, I. P., Kempton, J. B., and Withers, S. G. (1992) Inactivation of a β-glucosidase through the accumulation of a stable 2-deoxy-2-fluoro-α-D-glucopyranosyl-enzyme intermediate: a detailed investigation. *Biochemistry* **31,** 9970–9978
33. Lawson, S. L., Wakarchuk, W. W., and Withers, S. G. (1996) Effects of both shortening and lengthening the active site nucleophile of *Bacillus circulans* xylanase on catalytic activity. *Biochemistry* **35,** 10110–10118